University of Zurich[UZH]

Zurich Open Repository and Archive
University of Zurich
University Library
Strickhofstrasse 39
CH-8057 Zurich
www.zora.uzh.ch

Year: 2017

Cell Cycle-Dependent Kinase Cdk9 Is a Postexposure Drug Target against Human Adenoviruses

Prasad, Vibhu ; Suomalainen, Maarit ; Hemmi, Silvio ; Greber, Urs F

Abstract: Human adenoviruses (HAdVs) infect respiratory, gastrointestinal, and urinary tracts and give rise to eye infections and epidemic keratoconjunctivitis (EKC). They persist in lymphoid tissue and cause morbidity and mortality in immunocompromised people. Treatments with significant postexposure efficacy are not available. Here, we report that inhibition of the cell cycle-dependent kinase 9 (Cdk9) by RNA interference, or the compound flavopiridol, blocked infections with HAdV-C2/5, EKC-causing HAdV-D8/37, and progeny formation in human corneal epithelial and cancer cells. Flavopiridol abrogated the production of the immediate early viral transactivating protein E1A without affecting nuclear import of viral DNA. In morphometric plaque assays, the compound exhibited antiviral efficacy in both pre- and postexposure regimens with therapeutic indexes exceeding 10. The study identifies Cdk9 as a postexposure drug target against adenovirus infections in vitro and suggests that the clinically tested anticancer drug flavopiridol is a candidate for treating adenoviral EKC or adenovirus emergence upon immune suppression.

DOI: https://doi.org/10.1021/acsinfecdis.7b00009

Posted at the Zurich Open Repository and Archive, University of Zurich
ZORA URL: https://doi.org/10.5167/uzh-136948
Journal Article
Accepted Version

Originally published at:
Prasad, Vibhu; Suomalainen, Maarit; Hemmi, Silvio; Greber, Urs F (2017). Cell Cycle-Dependent Kinase Cdk9 Is a Postexposure Drug Target against Human Adenoviruses. ACS Infectious Diseases, 3(6):398-405.
DOI: https://doi.org/10.1021/acsinfecdis.7b00009

Cell cycle-dependent kinase Cdk9 is a post-exposure drug target against human adenoviruses

Vibhu Prasad[1, 2], Maarit Suomalainen[1], Silvio Hemmi[1], Urs F.Greber[1, 3]

1 Institute of Molecular Life Sciences, University of Zurich, Zurich, Switzerland

2 Molecular Life Sciences Graduate School, ETH and University of Zurich, Switzerland

3 corresponding author:
E-mail: urs.greber@imls.uzh.ch
Telephone: +41 44 635 48 41, Fax: +41 44 635 68 17

Keywords:
Epidemic keratoconjunctivitis (EKC); Impedance / xCELLigence; human adenovirus types C2, C5, D8, D37; host directed anti-viral compound; Flavopiridol, anti-viral compound

Running Title:
Cdk9 inhibitors against adenoviral EKC

Highlights

Cdk9 is a post-exposure drug target against a wide range of adenoviruses.

The clinical phase-IIB inhibitor of Cdk9 FLV blocks EKC-causing HAdV-D8 and HAdV-D37.

Abstract

Human adenoviruses (HAdVs) infect respiratory, gastrointestinal and urinary tracts, and give rise to eye infections and epidemic keratoconjunctivitis (EKC). They persist in lymphoid tissue, and cause morbidity and mortality in immunocompromised people. Treatments with significant post-exposure efficacy are not available. Here, we report that inhibition of the cell cycle-dependent kinase 9 (Cdk9) by RNA-interference, or the compound Flavopiridol blocked infections with HAdV-C2/5, EKC-causing HAdV-D8/37, and progeny formation in human corneal epithelial and cancer cells. Flavopiridol abrogated the production of the immediate early viral trans-activating protein E1A without affecting nuclear import of viral DNA. In morphometric plaque assays, the compound exhibited anti-viral efficacy in both pre- and post-exposure regimens with therapeutic indexes exceeding 10. The study identifies Cdk9 as a post-exposure drug target against adenovirus infections *in vitro,* and suggests that the clinically tested anti-cancer drug Flavopiridol is a candidate for treating adenoviral EKC, or adenovirus emergence upon immune suppression.

Introduction

Viral disease by recurrent or chronic agents, such as influenza virus, hepatitis viruses or HIV, or emerging agents, such as Ebola, Hanta or Zikavirus has had a long history and a strong impact on human evolution [1] [2]. This involves infections between humans, or between humans and animals in zoonotic and anthroponotic transmissions. Viral disease is difficult to combat because viruses subvert host defense, are genetically diverse, occur in large numbers, and readily evolve in response to environmental pressure.

Adenoviruses (AdVs) have evolved from bacteriophages. Today's adenoviruses are genetically distinct from bacteriophages, and infect most vertebrates. They are non-enveloped icosahedral particles with protruding fibers for cell attachment, and a pressurized DNA-protein core for stepwise uncoating, in response to cellular cues [3, 4]. More than 70 different human AdV (HAdV) serotypes and more than 70 additional human adenovirus genomes are known, and classified into 7 species (A-G) (see https://www.ncbi.nlm.nih.gov/Taxonomy/Browser/wwwtax.cgi?p=7&id=10508).
HAdVs replicate in the host nucleus and spread by lytic infection [5]. They cause a number of diseases, including respiratory and gastrointestinal disorders, as well as epidemic keratoconjunctivitis (EKC) [6]. Most diseases caused by AdV are self-limiting, due to strong innate and adaptive immunity, which provides protection against related serotypes [6-8]. In immunocompromised individuals, however, HAdV-species C (HAdV-C2/5) cause severe morbidity and mortality. Post-exposure adenovirus disease correlates with virus persistence and ongoing virus production in T-lymphocytes and primary human bronchial epithelial cells [7, 9].

Besides uncontrolled proliferation in immunocompromised individuals, adenoviral disease has additional unmet medical needs, such as EKC, which threatens eye vision, and causes large economic losses. Although antiviral agents, such as cidofovir and ribavirin have been used in oral or topical applications against HAdV, clinical success was limited due to narrow efficacy and toxicity [10]. Notably, ribavirin is inactive against HAdV-D8/19/37, the main agents causing EKC, and there are additional non-tested EKC-associated adenoviruses, including types 53, 54 and 56. Clinically approved anti-adenoviral drugs with significant post-exposure efficacy are not available.

Here, we provide *in vitro* evidence for post exposure efficacy of two clinically tested cell cycle dependent kinase (Cdk) inhibitors against EKC-causing HAdV types.

Flavopiridol (FLV) also known as Alvocidib, has previously been tested in phase-IIB clinical trials against leukemia. FLV is a semi-synthetic flavonoid compound inhibiting the cell cycle-dependent kinase Cdk9 with Ki of 3nM, and other Cdks, such as Cdk1, Cdk2, Cdk4, Cdk6, Cdk7 with Ki of 10nM-100nM [11]. It suppresses the replication of herpes simplex virus (HSV), human cytomegalovirus (HCMV) and human immune deficiency virus (HIV) [12]. FLV is clinically active against acute myeloid leukemia in combination therapy [13, 14]. CYC202 is a substituted purine analog, and inhibits Cdk2, Cdk7 and Cdk9. It is used to treat non-small cell lung cancer (NSCLC), Cushing's disease, leukemia, HIV and HSV infections, as well as chronic inflammation disorders [15]. Cdk9 controls transcriptional elongation. It forms a complex with cyclin T1, T2 or K, the so called positive transcription elongation factor beta P-TEFb, for a comprehensive review, see [11]. P-TEFb coordinates elongation after Pol II has been halted by DSIF (5,6-dichlorobenzimidazole 1-β-d-ribofuranoside-sensitivity-inducing factor) and NELF (negative elongation factor). P-TEFb phosphorylates DSIF and NELF, as well as the carboxy-terminal domain (CTD) of Pol II. This relieves repression, recruits the elongation complex, splicing and 3′-polyadenylation machineries, and enables transcription elongation.

Cdk9 enhances E1A transcription and HAdV-C5 infection through facilitating the recruitment of the Pol II mediator complex by the large E1A protein [16]. It has been suggested as an anti-viral target based on the notion that the broad Cdk9 inhibitor FIT-039, which inactivates other kinases, including Abl, IKKa, Rse and Rsk4 inhibited adenovirus replication measured by qPCR in cell-culture [17]. Here, we extend these data by showing that either FLV or the knock-down of Cdk9 inhibited the expression of the immediate early adenoviral protein E1A, and blocked the spreading of EKC-causing HAdV in post-exposure treatment, measured by live cell plaque assay and progeny titration.

Results and Discussion

Adenovirus infection is well known to drive the cells into S-phase, and thus enhance viral DNA replication [18]. We conducted a mini-drug screen with chemicals, which inhibit cell cycle progression or check points, and thereby arrest cells in particular cell cycle phases, or allow them to ignore stop signals and continue proliferation. To assess combinatorial effects of drugs and infection on toxicity we used ‘xCELLigence’ to measure cell impedance in real-time. xCELLigence provides label

free, real-time assessment of cell numbers, size, shape and substrate interaction, and a sensitive readout for cell toxicity [19]. Among the drugs tested in the mini-screen, the clearest effect on impedance was seen with FLV, which strongly reduced HAdV-C5 cell killing in a dose-dependent manner up to 125 nM (Fig. 1A, B). Representative impedance plots show cell indexes (CI) as a function of time, where FLV-treated cells infected with adenovirus showed a significant increase in CI compared to control infected cells (Fig. 1B). FLV inhibits a number of cell cycle dependent kinases, arrests cells in G1/S, and enhances apoptosis, for example upon genotoxic stress [11]. FLV was more effective at blocking HAdV cell killing than BMS-265246, a potent Cdk1/Cdk2 inhibitor arresting cells in G2 [20], or AZD-7762, which blocks checkpoint kinases and overrides DNA damage-induced cell cycle arrest [21], or CHIR-124, which inhibits the G2-M checkpoint [22] (see Fig. 1A).

Importantly, FLV inhibited HAdV-C5 infection, as shown by immunofluorescence staining of newly synthesized viral protein VI (Fig. 1C). FLV leads to a cell cycle arrest in G1/S by inhibition of cyclin D/Cdk4 and cyclin E/Cdk2 [11, 14]. We confirmed this notion with fluorescent ubiquitinated cell cycle indicator (FUCCI)-HeLa cells showing an enrichment of yellow G1/S cells upon FLV treatment at nanomolar concentrations for 24h (Fig. 1C). HeLa-FUCCI cells express green and red-fluorescent proteins fused to geminin (monomeric Azami Green labeled Geminin, dubbed as mAG-hGem), and Cdt1 (monomeric Kusabira orange fused to Cdt1, dubbed as mKO-Cdt1), respectively [23]. mAG-hGem undergoes proteasome-dependent degradation in G1 yielding red G1 cells, whereas cells in S, G2, and M phases are green, since Cdt1-RFP is ubiquitinated and degraded in these cell cycle phases. Early S-phase cells express both Cdt1 and geminin and appear yellow / orange, and in early G1, no fluorescence marker is expressed. As expected, HAdV-C5 infection enhanced the fraction of G1/S cells more than 2-fold to about 50%, compared to untreated, uninfected cells, which contained about 25% G1/S cells (Fig. 1C). Notably, FLV only slightly reduced the proportion of G1/S cells and lead to a small enhancement of S/G2/M cells upon infection. We conclude that FLV strongly inhibits adenovirus infection, and cell cycle progression.

Besides inhibiting the cell cycle, low nanomolar concentrations of FLV potently inactivate the positive transcription elongation factor beta (P-TEFb), and block most RNA Pol II (PolR2)-mediated transcription *in vivo* for a comprehensive review, see [11]. In human cells, the P-TEFb complex promotes elongation of the paused transcripts. It is composed of Cdk9 and cyclin T1, T2 or K depending on the cell type.

Elongation of early adenovirus transcripts has been shown to be dependent on Cdk9 recruitment to virus promoters [16]. We confirmed the importance of Cdk9 for HAdV infection by RNAi of Cdk9 which strongly reduced protein VI expression, in good correlation with Cdk9 knockdown (Fig. 1D). We found that adenovirus-infected HeLa cells increased the levels of PolR2A by a factor of about 11, as indicated by Western blots normalized to a-tubulin (Fig. 1E). Adenovirus-infected human diploid fibroblasts (HDF), which were immortalized with telomerase reverse transcriptase (TERT) likewise increased the PolR2A levels 1.9-fold compared to uninfected cells 24h pi (see later in Fig. 3C). This increase in PolR2A is in good agreement with earlier SILAC proteomics analyses, which found a 1.65 fold increase of PolR2A compared to control cells normalized to a-tubulin at 24h pi [24]. The C-terminal repeat domain (CTD) of PolR2A is a flexible scaffold for recruiting a variety of factors controlling RNA processing, and transcription elongation, including P-TEFb [25]. In agreement with the important role of Cdk9 in regulation of adenovirus transcription [17], FLV treatment at 125 nM completely blunted the induction of PolR2A by adenovirus, while not affecting the PolR2A levels of uninfected cells (Fig. 1E, and Fig. 3C). This suggests that FLV represses transcription in adenovirus-infected cells, in agreement with affecting the function of its target Cdk9 in transcription. In summary, FLV targets Cdk9, inhibits adenovirus infection, and maintains a large fraction of the infected cells in G1/S.

The first gene transcribed from the incoming viral genome is E1A. E1A proteins are natively unfolded. They promiscuously bind to a large range of host proteins, and activate viral and host gene transcription [18]. E1A transcription is subject to interferon-mediated repression, which can lead to persistent infections and repress lytic replication [9]. FLV at 63, 125 or 250 nM strongly suppressed E1A expression at 5h pi in HeLa-ATCC cells (Fig. 2A). E1A inhibition at 16h pi was much weaker than at 5h pi, when 63 nM or 125 nM of FLV was used. These results showed that despite continuous presence, FLV transiently inhibited the production of the immediate early viral gene product E1A, possibly by lowering the concentration of active P-TEFb. In contrast, essentially no E1A was detected up to 16h pi at 250 nM FLV.

We next tested if nuclear import of the incoming viral DNA (vDNA) was affected by FLV. Nuclear import of vDNA is a prerequisite for viral immediate early gene expression [18, 26]. Cells were infected with EdC-labeled HAdV-C5 with and without FLV, fixed 3.5h pi and immunostained for capsid protein hexon, and vDNA using click-chemistry, as described [26]. In all conditions viral capsids were found to be

associated with the infected cells (Fig. 2B). Quantification of the vDNA puncta over nuclei and within the cell boundaries showed that at average about 80% of the incoming capsid-free, uncoated vDNA localized to the nuclear area, without significant differences between control and FLV-treated cells (Fig. 2B). As expected there was large cell-to-cell variability, and some cells imported below 50% of the incoming vDNA. This indicates that FLV does not affect virus entry and nuclear import of vDNA at 3.5h pi.

We next tested the efficiency of FLV in blocking adenovirus infection post-exposure. HeLa-ATCC cells were infected with replication-competent HAdV-C2-dE3b_GFP for 24h. This virus enables the visualization of cell lysis and subsequent plaque formation by high-throughput microscopy [5]. FLV was then added for 24h, cells fixed, imaged by high-throughput microscopy and comets of infected cells quantified using Plaque 2.0 software [27]. Comets are amorphous plaques arising by virus spreading from a donor cell to neighboring cells in convection currents through the medium [5]. As shown in Fig. 2C, FLV slightly inhibited the formation of viral plaques at 63 nM, and completely abrogated plaque formation at 125 or 250 nM. This demonstrates that FLV is a potent adenovirus infection inhibitor with post-exposure efficacy. This conclusion was strengthened by the observation that the virus titers were equally reduced when FLV was added before virus entry or immediately post vDNA import into the nucleus at 4h pi (Fig. 2D). Similar results were obtained with human diploid fibroblasts immortalized with telomerase reverse transcriptase (HDF-TERT), or normal human fibroblasts WI38, which strongly attenuated adenovirus infection upon FLV treatment before or after virus entry (Fig. 3A, B, D). Infection inhibition of HDF-TERT was compatible with a block in viral transcription as suggested by the observation that FLV blunted PolR2A induction by adenovirus (Fig. 3C). We conclude that FLV inhibits adenovirus infection of HeLa and normal human fibroblasts after nuclear import of the viral genome.

So far, we have shown that the Cdk inhibitor FLV or the knock-down of Cdk9 inhibit infection of cancer cells and normal human fibroblasts with adenoviruses of the species C by inhibiting the production of E1A. We next tested the susceptibility of HAdV-C2-dE3b_GFP and epidemic keratoconjunctivitis (EKC)-causing species D adenoviruses to Cdk inhibitors in human corneal epithelial cells (HCE). FLV and Dinaciclib strongly target Cdk9, and have clinical activity in patients with chronic lymphocytic leukemia, and FLV appears to have a more narrow therapeutic index for

ovarian cancers in patients than Dinaciclib [14]. In addition to FLV, we tested CYC202, which has phase-IIB clinical data from lung and breast cancer clinical settings. CYC202 is a potent inhibitor of Cdk2/cyclin E, Cdk7/cyclin H, and Cdk5/p35 with submicromolar IC50 values. At higher micromolar concentrations, it leads to reduction of transcription, possibly via inhibition of Cdk7 and Cdk9 complexes. As a control, we included the PolR2 inhibitor DRB (5,6-dichlorobenzimidazole 1-β-d-ribofuranoside), which inhibits the initiation of RNA synthesis [28]. HCE cells were protected from infection with HAdV-C2-dE3b_GFP in presence of nanomolar concentrations of FLV, or micromolar concentrations of CYC202 or DRB (Fig. 4A, B). Likewise, infection of HCE cells with HAdV-D8 was strongly inhibited, indicated by immuno-staining of viral hexon and protein IIIa (Fig. 4C). Similar results were obtained with HAdV-D37 and HAdV-C2_dE3B_GFP (see Fig. 4D, and data not shown). We noticed a slight decrease in cell number upon FLV, CYC or DRB treatments for 24h. In case of FLV, this was due to cell cycle inhibition rather than toxicity as indicated by xCELLigence impedance measurements (Fig. 1C and Fig. 4D, F).

Dose-response curves for anti-viral efficacy and toxicity indicated therapeutic indexes (TI = LD_{50}/IC_{50}) of >10 for FLV in case of HAdV-D8/37 and C2, and TI between 3.6 and 10 for CYC202 and DRB (Fig. 4D). LC_{50} denotes the drug concentration with 50% cell lethality. Determination of virus titers produced at IC_{50} and IC_{90} concentrations of the inhibitors 48h pi showed very strong efficacy of FLV at 60 nM against HAdV-D8/37 and C2, and micromolar efficacy of CYC202 and DRB (Fig. 4E). Finally, to assess the dynamic drug-induced toxicity in HCE cells, we analyzed time-dependent LC_{50} for these inhibitors using xCELLigence. The results indicated that FLV, CYC202 and DRB were well tolerated with stable LC_{50} values even after 6 days of drug incubation (Fig. 4F). We conclude that the drugs unlikely inhibit adenovirus infection by general cell toxicity.

We had previously screened for factors enhancing adenovirus-induced cytotoxicity, and found that RNA silencing of Arf1 GTP exchange factor GBF1, or its chemical inhibition with Golgicide A (GCA) enhances adenovirus infection and killing [29]. The possibility of combining cytotoxicity triggered by cell cycle inhibition together with adenovirus infection prompted us to perform a small screen with cell cycle inhibitors, AZD-7762, BMS-265246, CHIR-124 and FLV. Instead of infection-enhancing effects, we found that cell cycle inhibitors impaired adenovirus infection in cell cultures, including infection of human cornea epithelial cells with EKC-causing adenovirus

types. Our study suggests that the transcription elongation factor Cdk9 is key for expression of the immediate early adenoviral protein E1A. E1A gene expression is indispensible for virus growth, and it also antagonizes interferon signaling and controls cell cycle progression [8, 9, 18]. E1A is regulated by an upstream enhancer region and a number of transcription factors, and signaling [3, 30]. In addition, the large E1A protein together with the mediator complex (MED) 26 and the elongation catalyst Cdk9 are important for E1A transcription [16]. Cdk9 is inhibited by nanomolar concentrations of FLV, and micromolar concentrations of CYC202 [14]. These conditions match the inhibitory profiles against adenovirus infections described here.

FLV has a unique mode of action by targeting Cdk9 of the P-TEFb complex and thereby inhibiting transcriptional elongation. FLV is particularly active in tumor cells that are sensitive to apoptosis inducers, such as chronic lymphocytic leukemia (CLL) and mantle cell lymphoma [14]. This is likely due to the fact that chronic lymphocyte leukemia cell survival is strongly dependent on anti-apoptotic proteins XIAP and Mcl-1, which are encoded by short-lived transcripts [31]. FLV reduces the abundance of short-lived unstable mRNAs. Notably, the adenoviral E1A transcripts are short-lived with a half-live of about 45 min [32]. The long E1A proteins are also short lived with a half live of a few hours [33]. We thus anticipate that E1A transcripts are subject to reduction by FLV. In fact, FLV inhibition of transcription is transient, for example, about 70% of the genes had reduced expression upon 300 nM FLV treatment within a few hours, although some genes showed enhanced expression, and cells recover from FLV treatment after about one day [11]. Such transient inhibition is sufficient to delay the production of E1A proteins (see Fig. 2). We speculate that Cdk9 in the P-TEFb complex cooperates with MED to enhance PolR2-mediated transcription and elongation of E1A mRNA. This coincides with our observation that PolR2 levels are enhanced in adenovirus infection, and suppressed by FLV. This scenario is in agreement with earlier proteomics data suggesting that E1A 13S is linked to MED23 [16]. Transcriptional activation of E1A through Cdk9 may enforce a positive feedback loop, and account for a strong enhancement of E1A expression early in adenovirus infection.

Our results also go along with the notion that transcription is controlled by factors negatively regulating elongation, such as DSIF and NELF, which are subject to inhibition by Cdk9 activity. Notably, DRB and FLV inhibit P-TEFb and mRNA production through impairment of transcription elongation [34]. This implies that Pol II is paused at promoter proximal sites, ready to receive activation signals (reviewed in

[11]). Projected to adenovirus, this may allow for rapid and synchronous activation of viral genomes in the nucleus, and help to overcome innate anti-viral networks.

The data here have implications for treating EKC-causing adenoviruses, and emerging adenoviruses upon immune-suppression. Viral EKC involves human adenoviruses of the species D [6], in particular the FLV-sensitive HAdV-D8, D19 and D37. FLV also inhibits HAdV-C5, which persistently infects human lymphoid cells, including T lymphocytes in tonsil and adenoid tissues, and rises to high titers in immunocompromised individuals [35]. The data here suggest that FLV and other Cdk9 inhibitors are potent candidates for development of topically applicable anti-adenoviral drugs against EKC. FLV can potentially be developed for treatment of viral emergence upon immune suppression owing to its rather broad anti-viral spectrum.

Methods

HCE cells immortalized with a recombinant SV40-adenovirus vector were kindly obtained from Dr. Karl Matter (University College London) [36]. HeLa-FUCCI cells kindly provided by Dr. Cornel Fraefel (University of Zurich) were grown on 96-well imaging plates (Greiner Biosciences), infected with HAdV-C5_wt at multiplicity-of-infection (moi) 1 in the presence of FLV (63 and 125 nM) and fixed with paraformaldehyde 18h pi. Nuclei were visualized with DAPI, and protein VI expression was used to estimate the infection efficiency [37]. Nuclear stain of DAPI was used to segment cells in different cell cycle stages using Cell Profiler Analyst software and Machine Learning Algorithms [5, 27, 29, 38]. HeLa-FUCCI cells express mKO-Cdt1 (orange, G1 phase), and mAG-hGem (green, S/G2/M phase). A small gap in fluorescence change from red to green indicates a G1/S transition [23]. The customized software differentiated between G1, G1/S and S/G2/M cells. Procedures describing viruses, cells, transfections, xCELLigence, click chemistry for viral DNA detection have been described before [26, 29, 37, 39].

Detailed methods are described in the Supporting Information file: 1) Cell lines and viruses. 2) Transfection, drug inhibition, infection. 3) xCELLigence. 4) Western blotting. 5) Scoring of cells in different cell cycle phases using Machine Learning. 6) Click chemistry and visualization of single viral DNA dots. 6) Virus growth assay. 7) Supporting references.

Author Contributions

Conceived project (UFG, VP), performed experiments (VP), analyzed data (VP, MS, SH, UFG), wrote manuscript (VP, MS, UFG).

Acknowledgements

The work was supported by a grant from the Swiss National Science Foundation to UFG (SNSF 310030B_160316). We are grateful to Dr. Karl Matter and Dr. Niklas Arnberg for human cornea epithelial cells, and Dr. David Price for discussions.

Figure Legends

Fig. 1: Knock-down or chemical inhibition of Cdk9 inhibits HAdV infection

(A) Effects of cell-cycle inhibitors on adenovirus-induced cytotoxicity measured with xCELLigence. CIT50 is the time-point when the impedance readout (Cell Index, CI) reaches 50% of maximum impedance of control (DMSO) cells. ΔCIT50 is the difference between CIT50 of drug-treated and control cells. The higher the ΔCIT50 values are, the stronger is the inhibition of infection. The plot shows a linear correlation of ΔCIT50 and FLV dose up to 125 nM. Note that the effects of BMS (Bristol-Myer Squib)-265246, AZD (AstraZeneca)-7762 and CHIR (Chirion)-124, which primarily affect the cell cycle, have small effects on increasing the ΔCIT_{50} values.

(B) Representative CI profiles for FLV inhibition of adenovirus infection determined by xCELLigence. Drug was added together with the virus. The horizontal dashed line indicates CI50 of control cells.

(C) Cell cycle analyses in presence of FLV and HAdV. HeLa-FUCCI cells were incubated with FLV in presence or absence of HAdV-C5-wt (moi 1) for 24h, fixed and analyzed for infection by anti-protein VI immuno-staining. The zoomed-in regions indicate cells in G1 (red), G1/S (yellow) and S/G2/M (green) phases of cell-cycle. Quantification of cells in different cell-cycle phases was performed using Cell Profiler. These results imply that the G1/S cell cycle inhibitor FLV does not affect the cell cycle control exerted by adenovirus.

(D) HeLa-ATCC cells were transfected with siRNA against Cdk9 or scrambled (NT) for 48h as described [40], infected with HAdV-C2-dE3b_GFP for 18h, fixed and probed for infection using anti-protein VI antibody. Mean and SEM values are shown from two technical replicates of a representative experiment and the experiment was repeated two times. Levels of Cdk9 were determined by Western blotting using beta-tubulin as loading control.

(E) Total RNAP2A levels are enhanced in adenovirus-infected HeLa-ATCC cells. Cells were infected with HAdV-C2-dE3b_GFP in the presence of FLV for 24h, lysed and analyzed by Western blotting for RNAP2A levels using an antibody against the CTD (Abcam ab817). PolR2A levels relative to alpha-tubulin are indicated, including SEM from two independent experiments.

Fig. 2: Flavopiridol inhibits early viral gene expression but not nuclear genome import

(A) FLV delays the production of E1A proteins in adenovirus infected HeLa-ATCC cells. Cells were infected with HAdV-C5 in presence or absence of FLV and E1A levels were determined by Western blots at 5 and 16h pi using beta-tubulin as loading control. One of three representative experiments is shown.

(B) No effect of FLV on virus association with cells and nuclear import of vDNA. HeLa-ATCC cells were incubated with EdC-labeled HAdV-C5, fixed 3.5h pi and probed for viral-DNA by copper-catalyzed click chemistry. Viral capsids were stained with anti-hexon antibody and imaged with a Leica SP8 upright confocal microscope. Distribution of single viral genomes in nuclei and cytoplasm was assessed by segmenting the maximal projections of images using Cell Profiler. Nuclear capsid-free vDNA dots normalized to the total vDNA are shown per cell.

(C) FLV inhibits adenovirus infection post-exposure. A549 cells were incubated with HAdV-C2-dE3b_GFP (moi 0.0008) for 24h, followed by addition of FLV for 24h. Samples were fixed, DAPI-stained, imaged by high-throughput microscopy and analysed for viral plaques using Plaque 2.0.

(D) Post-entry anti-viral efficacy of FLV. HeLa-ATCC cells were infected with HAdV-C2-dE3b_GFP for 1h, washed, incubated with FLV, or without FLV for 3h, followed by FLV addition at 4h pi. At 48h pi, virus titers in the combined cell and supernatant fractions were determined on HeLa-ATCC cells using GFP as a readout 18h pi. The mean numbers of GFP-positive cells are shown including SEM from two replicates of a representative experiment, and the experiment was repeated two times.

Fig. 3: Cdk-targeting agents inhibit EKC-causing adenoviruses in normal human cells

(A) HDF-TERT cells were infected with HAdV-C2-dE3b_GFP in the presence of FLV, fixed at 24h pi, immuno-stained for viral E1A proteins, and analyzed using Cell Profiler. Mean and SEM values are shown from two replicates of a representative experiment and the experiment was repeated two times.

(B) Post-entry anti-viral efficacy of FLV in HDF-TERT cells. Cells were inoculated with viruses for 1h, followed by washing and addition of FLV 4h pi. At 72h pi, cell- and supernatant-associated viruses were titered on HeLa-ATCC cells using GFP as a readout 18h pi. The mean numbers of GFP positive cells are shown including SEM from two replicates of a representative experiment and the experiment was repeated two times.

(C) Total RNAP2A levels are enhanced in adenovirus-infected HDF-TERT cells. Experiment was conducted as described in Fig. 1E. PolR2A levels relative to alpha-tubulin are indicated, including SEM from two independent experiments.

(D) FLV blocks adenovirus-induced cytopathic effects in WI38 cells. Cells were infected with HAdV-D37 in the presence of FLV (added 4h pi) and analyzed by differential interference contrast imaging 48h pi.

Fig. 4: Cdk-targeting agents inhibit EKC-causing adenovirus in HCE cells

(A, B) HCE cells were infected with HAdV-C2-dE3b_GFP in the presence of IC_{50} and IC_{90} amounts of FLV, CYC202 (CYC) and DRB, fixed at 24h pi, and immuno-stained for viral proteins E1A and protein VI. Mean and SEM values are shown from two replicates of a representative experiment and the experiment was repeated two times.

(C) Immunofluorescence staining against hexon and protein IIIa shows inhibition of HCE infection with the EKC-causing adenovirus serotype HAdV-D8 in presence of nanomolar concentrations of FLV.

(D) Infection inhibition and cell toxicity profiles of FLV, CYC202 and DRB. The 50% efficiency of infection inhibition (IC50) has been determined using anti-hexon immunofluorescence, and 50% cellular toxicity levels (CI_{50}) were determined from CI measurements with xCELLigence. Relative cell viability is indicated as $1 – [(CI_{no\ drug} – CI_{drug})/CI_{no\ drug}]$. The table shows the therapeutic indexes ($TI = CI_{50}/IC_{50}$) of FLV, CYC202 and DRB for HAdV-C2, HAdV-D8 and HAdV-D37.

(E) Estimation of viral titers at IC50 and IC90 values of FLV, CYC202 and DRB in HAdV-C2, D8 and D37 infected HCE cells. Cells were inoculated with viruses in the presence of indicated drugs, progeny particles collected at 48h pi, and titers of

viruses determined on HeLa-ATCC cells by counting the anti-hexon positive cells 18h pi. Mean and SEM values from two experiments are shown.

(F) Real-time toxicity measurement of FLV, CYC202 and DRB in HCE cells for up to 6 days post treatment. Cells were seeded on xCELLigence E-well plates, drugs added 56h post seeding, and CI measured at intervals of 15 min. CI50 values were estimated at each of these intervals, and plotted against time. Horizontal dotted lines indicate the average CI50 values over the entire period. Green and red lines indicate two time-points from FLV-treated cells at 80 and 130h post treatment, respectively.

References

[1] Lederberg, J. (2000) Infectious history, *Science 288*, 287-293.

[2] Greber, U. F., and Bartenschlager, R. (2017) Editorial: An expanded view of viruses, *FEMS microbiology reviews 41*, 1-4. doi: 10.1093/femsre/fuw044.

[3] Wolfrum, N., and Greber, U. F. (2013) Adenovirus signalling in entry, *Cell Microbiol 15*, 53-62. doi: 10.1111/cmi.12053.

[4] Yamauchi, Y., and Greber, U. F. (2016) Principles of Virus Uncoating: Cues and the Snooker Ball, *Traffic 17*, 569-592. doi: 10.1111/tra.12387.

[5] Yakimovich, A., Gumpert, H., Burckhardt, C. J., Lutschg, V. A., Jurgeit, A., Sbalzarini, I. F., and Greber, U. F. (2012) Cell-free transmission of human adenovirus by passive mass transfer in cell culture simulated in a computer model, *J Virol 86*, 10123–10137. doi: 10.1128/JVI.01102-12.

[6] Lenaerts, L., De Clercq, E., and Naesens, L. (2008) Clinical features and treatment of adenovirus infections, *Rev Med Virol 18*, 357-374. doi: 10.1002/rmv.589.

[7] Lion, T. (2014) Adenovirus infections in immunocompetent and immunocompromised patients, *Clinical Microbiology Reviews 27*, 441-462. doi: 10.1128/CMR.00116-13.

[8] Hendrickx, R., Stichling, N., Koelen, J., Kuryk, L., Lipiec, A., and Greber, U. F. (2014) Innate Immunity to Adenovirus, *Hum Gene Ther 25*, 265–284. doi: 10.1089/hum.2014.001.

[9] Zheng, Y., Stamminger, T., and Hearing, P. (2016) E2F/Rb Family Proteins Mediate Interferon Induced Repression of Adenovirus Immediate Early Transcription to Promote Persistent Viral Infection, *PLoS Pathog 12*, e1005415. doi: 10.1371/journal.ppat.1005415.

[10] Kinchington, P. R., Romanowski, E. G., and Gordon, Y. J. (2005) Prospects for adenovirus antivirals, *Journal of Antimicrobial Chemotherapy 55*, 424-429.

[11] Guo, J., and Price, D. H. (2013) RNA polymerase II transcription elongation control, *Chem Rev 113*, 8583-8603. doi: 10.1021/cr400105n.

[12] Schang, L. M., St Vincent, M. R., and Lacasse, J. J. (2006) Five years of progress on cyclin-dependent kinases and other cellular proteins as potential targets for antiviral drugs, *Antivir Chem Chemother 17*, 293-320.

[13] Zeidner, J. F., and Karp, J. E. (2015) Clinical activity of alvocidib (flavopiridol) in acute myeloid leukemia, *Leukemia research 39*, 1312-1318. doi: 10.1016/j.leukres.2015.10.010.

[14] Asghar, U., Witkiewicz, A. K., Turner, N. C., and Knudsen, E. S. (2015) The history and future of targeting cyclin-dependent kinases in cancer therapy, *Nat Rev Drug Discov 14*, 130-146. doi: 10.1038/nrd4504.

[15] MacCallum, D. E., Melville, J., Frame, S., Watt, K., Anderson, S., Gianella-Borradori, A., Lane, D. P., and Green, S. R. (2005) Seliciclib (CYC202, R-Roscovitine) induces cell death in multiple myeloma cells by inhibition of RNA polymerase II-dependent transcription and down-regulation of Mcl-1, *Cancer Res 65*, 5399-5407. doi: 10.1158/0008-5472.CAN-05-0233.

[16] Vijayalingam, S., and Chinnadurai, G. (2013) Adenovirus L-E1A activates transcription through mediator complex-dependent recruitment of the super elongation complex, *J Virol 87*, 3425-3434. doi: 10.1128/JVI.03046-12.

[17] Yamamoto, M., Onogi, H., Kii, I., Yoshida, S., Iida, K., Sakai, H., Abe, M., Tsubota, T., Ito, N., Hosoya, T., and Hagiwara, M. (2014) CDK9 inhibitor FIT-039 prevents replication of multiple DNA viruses, *J Clin Invest 124*, 3479-3488. doi: 10.1172/JCI73805.

[18] Berk, A. J. (2005) Recent lessons in gene expression, cell cycle control, and cell biology from adenovirus, *Oncogene 24*, 7673-7685.

[19] O'Connell, J., Abassi, Y. A., Xi, B., Wang, X., and Xu, X. (2008) Real-time cell-based toxicology testing might replace animal testing for product release and drug safety, *Biochemica 4*, 11-13.

[20] Misra, R. N., Xiao, H., Rawlins, D. B., Shan, W., Kellar, K. A., Mulheron, J. G., Sack, J. S., Tokarski, J. S., Kimball, S. D., and Webster, K. R. (2003) 1H-Pyrazolo[3,4-b]pyridine inhibitors of cyclin-dependent kinases: highly potent 2,6-Difluorophenacyl analogues, *Bioorg Med Chem Lett 13*, 2405-2408.

[21] Zabludoff, S. D., Deng, C., Grondine, M. R., Sheehy, A. M., Ashwell, S., Caleb, B. L., Green, S., Haye, H. R., Horn, C. L., Janetka, J. W., Liu, D., Mouchet, E., Ready, S., Rosenthal, J. L., Queva, C., Schwartz, G. K., Taylor, K. J., Tse, A. N., Walker, G. E., and White, A. M. (2008) AZD7762, a novel checkpoint kinase inhibitor, drives checkpoint abrogation and potentiates DNA-targeted therapies, *Mol Cancer Ther 7*, 2955-2966. doi: 10.1158/1535-7163.MCT-08-0492.

[22] Tse, A. N., Rendahl, K. G., Sheikh, T., Cheema, H., Aardalen, K., Embry, M., Ma, S., Moler, E. J., Ni, Z. J., Lopes de Menezes, D. E., Hibner, B., Gesner, T. G., and Schwartz, G. K. (2007) CHIR-124, a novel potent inhibitor of Chk1, potentiates the cytotoxicity of topoisomerase I poisons in vitro and in vivo, *Clin Cancer Res 13*, 591-602. doi: 10.1158/1078-0432.CCR-06-1424.

[23] Sakaue-Sawano, A., Kurokawa, H., Morimura, T., Hanyu, A., Hama, H., Osawa, H., Kashiwagi, S., Fukami, K., Miyata, T., Miyoshi, H., Imamura, T., Ogawa, M., Masai, H., and Miyawaki, A. (2008) Visualizing spatiotemporal dynamics of multicellular cell-cycle progression, *Cell 132*, 487-498. doi: 10.1016/j.cell.2007.12.033.

[24] Evans, V. C., Barker, G., Heesom, K. J., Fan, J., Bessant, C., and Matthews, D. A. (2012) De novo derivation of proteomes from transcriptomes for transcript and protein identification, *Nat Methods 9*, 1207-1211. doi: 10.1038/nmeth.2227.

[25] Phatnani, H. P., and Greenleaf, A. L. (2006) Phosphorylation and functions of the RNA polymerase II CTD, *Genes Dev 20*, 2922-2936. doi: 10.1101/gad.1477006.

[26] Wang, I. H., Suomalainen, M., Andriasyan, V., Kilcher, S., Mercer, J., Neef, A., Luedtke, N. W., and Greber, U. F. (2013) Tracking viral genomes in host cells at single-molecule resolution, *Cell Host Microbe 14*, 468-480. doi: 10.1016/j.chom.2013.09.004.

[27] Yakimovich, A., Andriasyan, V., Witte, R., Wang, I. H., Prasad, V., Suomalainen, M., and Greber, U. F. (2015) Plaque2.0-A High-Throughput Analysis Framework to Score Virus-Cell Transmission and Clonal Cell Expansion, *PLoS One 10*, e0138760. doi: 10.1371/journal.pone.0138760.

[28] Sehgal, P. B., Darnell, J. E., Jr., and Tamm, I. (1976) The inhibition by DRB (5,6-dichloro-1-beta-D-ribofuranosylbenzimidazole) of hnRNA and mRNA production in HeLa cells, *Cell 9*, 473-480.

[29] Prasad, V., Suomalainen, M., Pennauer, M., Yakimovich, A., Andriasyan, V., Hemmi, S., and Greber, U. F. (2014) Chemical Induction of Unfolded Protein Response Enhances Cancer Cell Killing through Lytic Virus Infection, *J Virol 88*, 13086-13098. doi: 10.1128/JVI.02156-14.

[30] Frisch, S. M., and Mymryk, J. S. (2002) Adenovirus-5 E1A: paradox and paradigm, *Nat Rev Mol Cell Biol 3*, 441-452.

[31] Chen, R., Keating, M. J., Gandhi, V., and Plunkett, W. (2005) Transcription inhibition by flavopiridol: mechanism of chronic lymphocytic leukemia cell death, *Blood 106*, 2513-2519. doi: 10.1182/blood-2005-04-1678.

[32] Spindler, K. R., and Berk, A. J. (1984) Rapid intracellular turnover of adenovirus 5 early region 1A proteins, *J Virol 52*, 706-710.

[33] Slavicek, J. M., Jones, N. C., and Richter, J. D. (1988) Rapid turnover of adenovirus E1A is determined through a co-translational mechanism that requires an aminoterminal domain, *EMBO J 7*, 3171-3180.

[34] Chodosh, L. A., Fire, A., Samuels, M., and Sharp, P. A. (1989) 5,6-Dichloro-1-beta-D-ribofuranosylbenzimidazole inhibits transcription elongation by RNA polymerase II in vitro, *J Biol Chem 264*, 2250-2257.

[35] Garnett, C. T., Talekar, G., Mahr, J. A., Huang, W., Zhang, Y., Ornelles, D. A., and Gooding, L. R. (2009) Latent species C adenoviruses in human tonsil tissues, *J Virol 83*, 2417-2428. doi: 10.1128/JVI.02392-08.

[36] Araki-Sasaki, K., Ohashi, Y., Sasabe, T., Hayashi, K., Watanabe, H., Tano, Y., and Handa, H. (1995) An SV40-immortalized human corneal epithelial cell line and its characterization, *Invest Ophthalmol Vis Sci 36*, 614-621.

[37] Burckhardt, C. J., Suomalainen, M., Schoenenberger, P., Boucke, K., Hemmi, S., and Greber, U. F. (2011) Drifting motions of the adenovirus receptor CAR and immobile integrins initiate virus uncoating and membrane lytic protein exposure, *Cell Host Microbe 10*, 105-117. doi: 10.1016/j.chom.2011.07.006.

[38] Jones, T., Kang, I., Wheeler, D., Lindquist, R., Papallo, A., Sabatini, D., Golland, P., and Carpenter, A. (2008) CellProfiler Analyst: data exploration and analysis software for complex image-based screens, In *BMC Bioinformatics 2008 9:1*, p 1, BioMed Central.

[39] Nagel, H., Maag, S., Tassis, A., Nestle, F. O., Greber, U. F., and Hemmi, S. (2003) The alphavbeta5 integrin of hematopoietic and nonhematopoietic cells is a transduction receptor of RGD-4C fiber-modified adenoviruses, *Gene Ther 10*, 1643-1653. doi: 10.1038/sj.gt.3302058.

[40] Luisoni, S., Suomalainen, M., Boucke, K., Tanner, L. B., Wenk, M. R., Guan, X. L., Grzybek, M., Coskun, U., and Greber, U. F. (2015) Co-option of Membrane Wounding Enables Virus Penetration into Cells, *Cell Host Microbe 18*, 75-85. doi: 10.1016/j.chom.2015.06.006.

F1

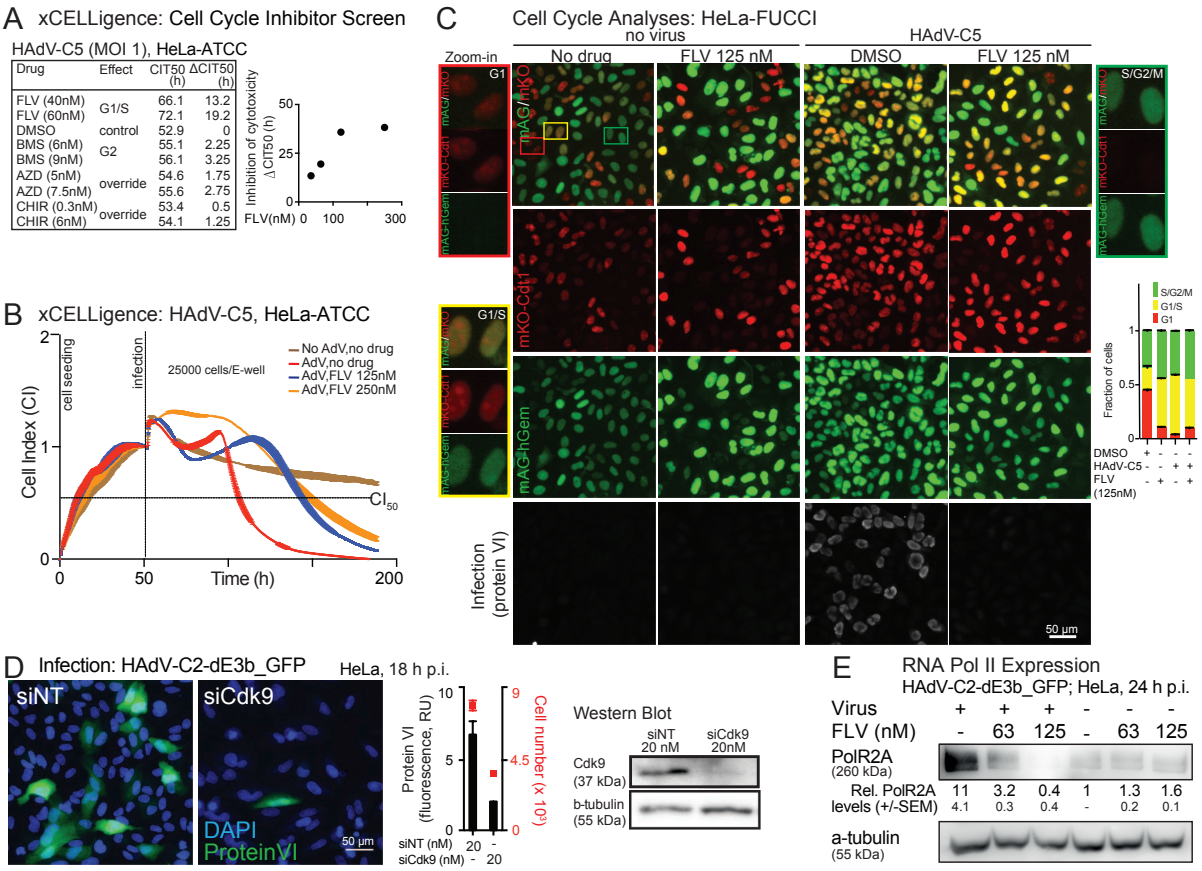
A xCELLigence: Cell Cycle Inhibitor Screen
HAdV-C5 (MOI 1), HeLa-ATCC
Drug | Effect | CIT50 (h) | ΔCIT50 (h)
FLV (40nM) | G1/S | 66.1 | 13.2
FLV (60nM) | | 72.1 | 19.2
DMSO | control | 52.9 | 0
BMS (6nM) | G2 | 55.1 | 2.25
BMS (9nM) | | 56.1 | 3.25
AZD (5nM) | override | 54.6 | 1.75
AZD (7.5nM) | | 55.6 | 2.75
CHIR (0.3nM) | override | 53.4 | 0.5
CHIR (6nM) | | 54.1 | 1.25
Inhibition of cytotoxicity Δ CIT50 (h)
FLV(nM) 0 100 300
B xCELLigence: HAdV-C5, HeLa-ATCC
Cell Index (CI)
cell seeding
infection
25000 cells/E-well
No AdV,no drug
AdV,no drug
AdV,FLV 125nM
AdV,FLV 250nM
CI50
Time (h)
C Cell Cycle Analyses: HeLa-FUCCI
no virus
HAdV-C5
Zoom-in
No drug
FLV 125 nM
DMSO
FLV 125 nM
G1
S/G2/M
G1/S
mAG-hGem
mKO-Cdt1
Infection (protein VI)
50 µm
S/G2/M
G1/S
G1
Fraction of cells
DMSO
HAdV-C5
FLV (125nM)
D Infection: HAdV-C2-dE3b_GFP
HeLa, 18 h p.i.
siNT
siCdk9
DAPI
ProteinVI
50 µm
Protein VI (fluorescence, RU)
Cell number (x 10³)
siNT (nM) 20 -
siCdk9 (nM) - 20
Western Blot
siNT 20 nM
siCdk9 20nM
Cdk9 (37 kDa)
b-tubulin (55 kDa)
E RNA Pol II Expression
HAdV-C2-dE3b_GFP; HeLa, 24 h p.i.
Virus + + + - - -
FLV (nM) - 63 125 - 63 125
PolR2A (260 kDa)
Rel. PolR2A levels (+/-SEM) 11 4.1 | 3.2 0.3 | 0.4 0.4 | 1 - | 1.3 0.2 | 1.6 0.1
a-tubulin (55 kDa)

F2

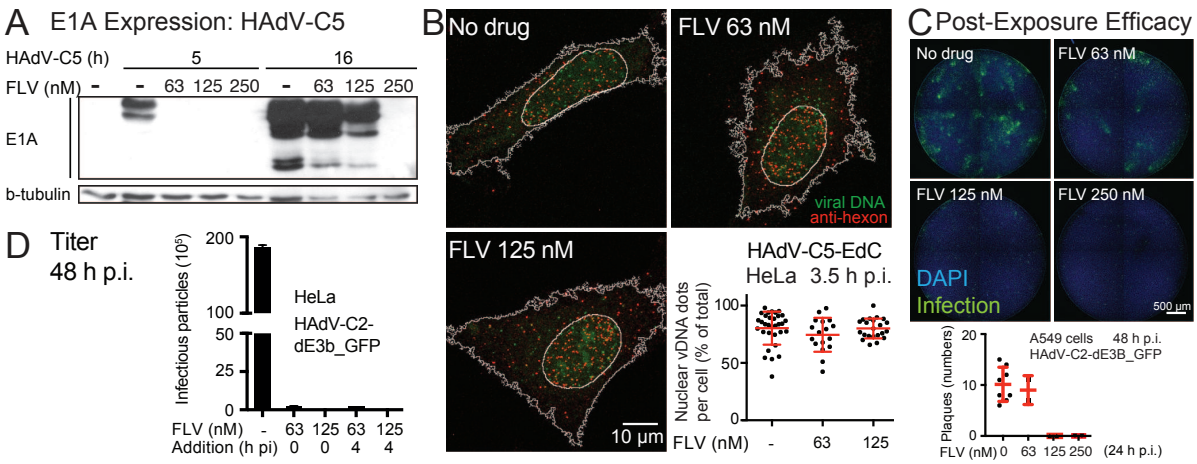
A E1A Expression: HAdV-C5
HAdV-C5 (h)
5
16
FLV (nM) - - 63 125 250 - 63 125 250
E1A
b-tubulin
B
No drug
FLV 63 nM
viral DNA
anti-hexon
FLV 125 nM
10 µm
HAdV-C5-EdC
HeLa 3.5 h p.i.
Nuclear vDNA dots per cell (% of total)
100
50
0
FLV (nM) - 63 125
C Post-Exposure Efficacy
No drug
FLV 63 nM
FLV 125 nM
FLV 250 nM
DAPI
Infection
500 µm
A549 cells 48 h p.i.
HAdV-C2-dE3B_GFP
Plaques (numbers)
20
10
0
FLV (nM) 0 63 125 250 (24 h p.i.)
D Titer
48 h p.i.
Infectious particles (10^5)
200
100
50
25
0
HeLa
HAdV-C2-dE3b_GFP
FLV (nM) - 63 125 63 125
Addition (h pi) 0 0 4 4

F3

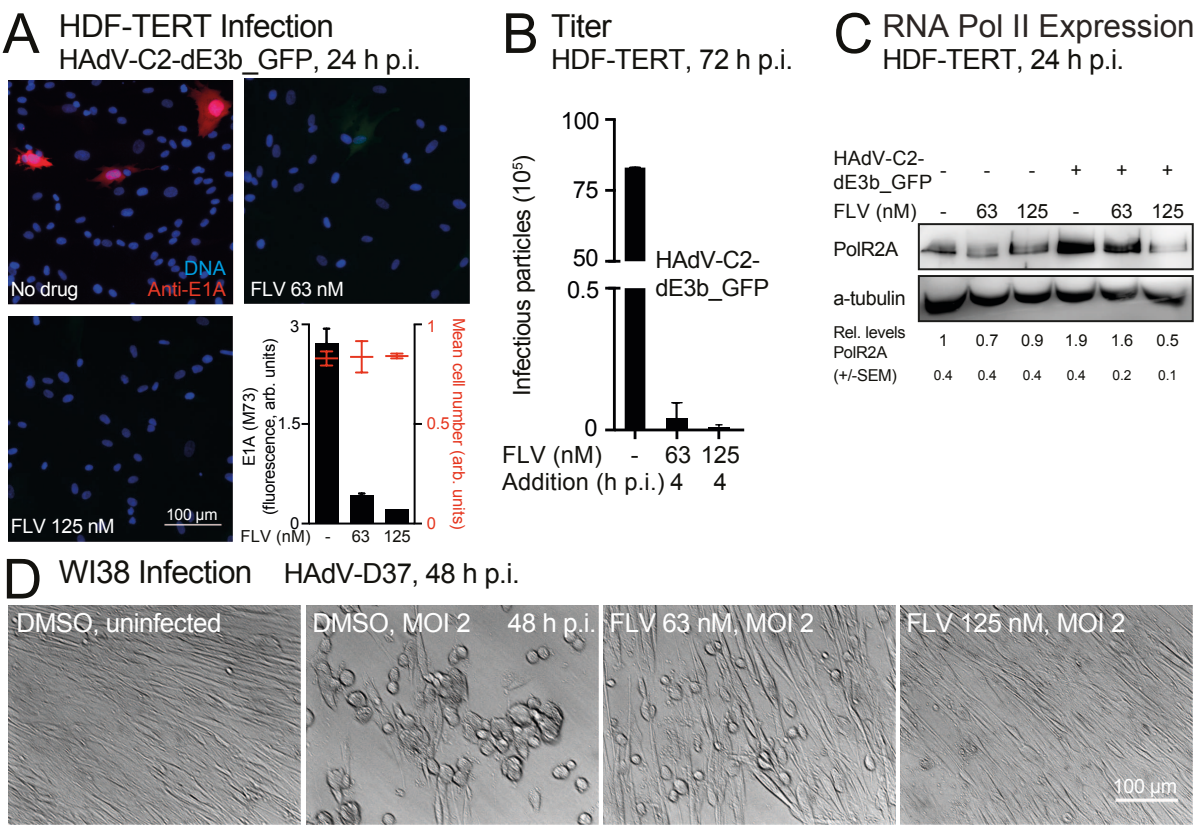
A
HDF-TERT Infection
HAdV-C2-dE3b_GFP, 24 h p.i.
No drug
DNA
Anti-E1A
FLV 63 nM
FLV 125 nM
100 µm
E1A (M73)
(fluorescence, arb. units)
Mean cell number (arb. units)
FLV (nM) - 63 125
B
Titer
HDF-TERT, 72 h p.i.
Infectious particles (10^5)
HAdV-C2-
dE3b_GFP
FLV (nM) - 63 125
Addition (h p.i.) 4 4
C
RNA Pol II Expression
HDF-TERT, 24 h p.i.
HAdV-C2-
dE3b_GFP - - - + + +
FLV (nM) - 63 125 - 63 125
PolR2A
a-tubulin
Rel. levels
PolR2A 1 0.7 0.9 1.9 1.6 0.5
(+/-SEM) 0.4 0.4 0.4 0.4 0.2 0.1

D
WI38 Infection
HAdV-D37, 48 h p.i.
DMSO, uninfected
DMSO, MOI 2
48 h p.i.
FLV 63 nM, MOI 2
FLV 125 nM, MOI 2
100 µm

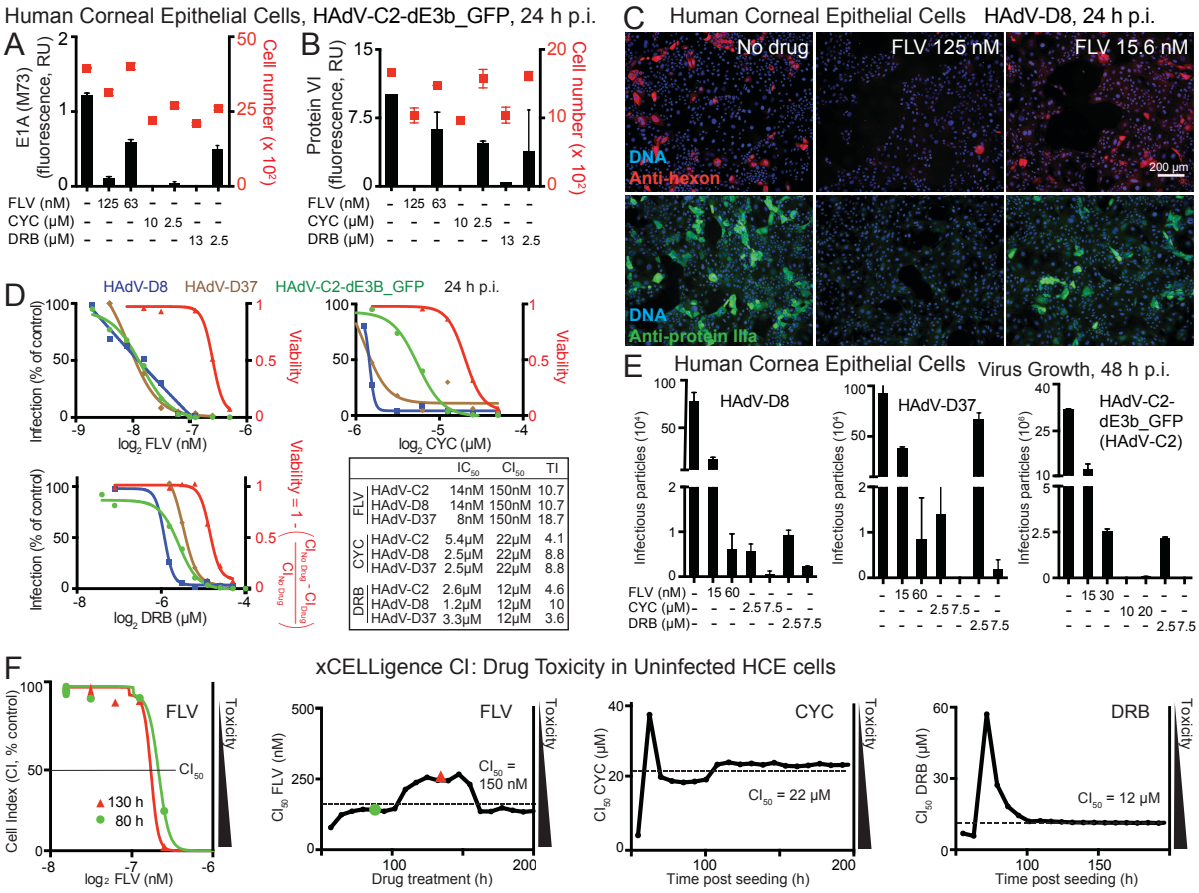
Human Corneal Epithelial Cells, HAdV-C2-dE3b_GFP, 24 h p.i.
A
E1A (M73) (fluorescence, RU)
Cell number (x 10²)
FLV (nM) - 125 63 - - - -
CYC (μM) - - - 10 2.5 - -
DRB (μM) - - - - - 13 2.5
B
Protein VI (fluorescence, RU)
Cell number (x 10²)
FLV (nM) - 125 63 - - - -
CYC (μM) - - - 10 2.5 - -
DRB (μM) - - - - - 13 2.5
C Human Corneal Epithelial Cells HAdV-D8, 24 h p.i.
No drug
FLV 125 nM
FLV 15.6 nM
DNA
Anti-hexon
200 μm
DNA
Anti-protein IIIa
D
HAdV-D8 HAdV-D37 HAdV-C2-dE3B_GFP 24 h p.i.
Infection (% of control)
Viability
log2 FLV (nM)
log2 CYC (μM)
log2 DRB (μM)
Viability = 1 - (CINo Drug - CIDrug / CINo Drug)
IC50 CI50 TI
FLV HAdV-C2 14nM 150nM 10.7
HAdV-D8 14nM 150nM 10.7
HAdV-D37 8nM 150nM 18.7
CYC HAdV-C2 5.4μM 22μM 4.1
HAdV-D8 2.5μM 22μM 8.8
HAdV-D37 2.5μM 22μM 8.8
DRB HAdV-C2 2.6μM 12μM 4.6
HAdV-D8 1.2μM 12μM 10
HAdV-D37 3.3μM 12μM 3.6
E Human Cornea Epithelial Cells Virus Growth, 48 h p.i.
HAdV-D8
HAdV-D37
HAdV-C2-dE3b_GFP (HAdV-C2)
Infectious particles (10⁴)
Infectious particles (10⁶)
FLV (nM) - 15 60 - - - -
CYC (μM) - - - 2.5 7.5 - -
DRB (μM) - - - - - 2.5 7.5
F
xCELLigence CI: Drug Toxicity in Uninfected HCE cells
Cell Index (CI, % control)
FLV
CI50
130 h
80 h
log2 FLV (nM)
Toxicity
CI50 FLV (nM)
CI50 = 150 nM
Drug treatment (h)
CI50 CYC (μM)
CYC
CI50 = 22 μM
Time post seeding (h)
CI50 DRB (μM)
DRB
CI50 = 12 μM
Time post seeding (h)

Supporting Information for:

Cell cycle-dependent kinase Cdk9 is a post-exposure drug target against human adenoviruses

Vibhu Prasad, Maarit Suomalainen, Silvio Hemmi, Urs F.Greber

Number of pages: 6

Number of figures: 0

Number of tables: 0

Contents

Cell lines and viruses

HeLa-ATCC and A549 (American Type Culture Collection, ATCC), human corneal epithelial (HCE) cells were obtained from Dr. Niklas Arnberg (UMEA University, Sweden) were grown at 37˚C in 5% CO_2 environment in Dulbecco's modified Eagle's medium (DMEM; Sigma) supplemented with 7.5% fetal calf serum (FCS; Life Technologies), as described [1]. Replicating wild type HAdV-C5 (HAdV-C5_wt) and HAdV-C2-dE3b_GFP were grown in A549 cells as described before [2, 3]. Major EKC-causing adenovirus serotypes D8 and D37 were plaque purified and amplified in A549 cells as described for HAdV-C2 [4].

Transfection, drug inhibition, infection

Quantification of infections after drug treatment and siRNA transfections were performed in 96-well plate format. Small-interfering RNA (siRNA; ON-TARGET Plus SMARTPool; Dharmacon) transfection experiments and drug treatments were done exactly as described previously [5]. All drug incubations were done at the time of addition of virus, and the cells were fixed at indicated time points pi. Antibodies used for immunofluorescence were against protein-VI [6], hexon (Mab8251 pan-adeno, Abcam) and protein-IIIa [7]. For post exposure experiments, FLV was added 24h pi.

xCELLigence

xCelligence system (Roche Appliced Science and ACEA Biosciences) used for quantifying HAdV cytotoxicity was done exactly as described [5]. For estimation of long-term toxicity effects of drugs, cells were grown on E-view plates for 48h, and serial dilutions of drugs were added. CI was recorded every 15 min and drug concentrations at which the CI dropped to 50% of untreated cells (CI_{50}) was plotted for all time points. Using this pipeline, the long-term effect of drugs was monitored until 6 days post seeding. The average value was taken as a toxicity index for the different drugs.

Western blotting

HeLa-ATCC cells were grown in 24-well plates and infected with HAdV-C5-wt multiplicity of infection (moi) 200 in the presence of FLV (63, 125 and 250 nM) at 37˚C for 5 and 16h, and cell extracts were collected in lysis buffer (0.2 ml of 200 mM Tris, pH 8.8, 20% glycerol, 5 mM EDTA, 50 mM DTT, 5% SDS, 0.02% bromophenol blue), boiled at 95˚C for 5 min and sheared through G21 needles (Sterican). Proteins were resolved on 15% polyacrylamide gels, transferred to a poly-vinylidene-difluoride membrane (Amersham) and blocked with 5% milk powder. Proteins were detected using anti-E1A M73 (Millipore 05-599), anti-PolR2A CTD (Abcam, ab817), anti-α-tubulin (Sigma T-9026) and ß-tubulin (Amersham).

Scoring of cells in different cell cycle phases using Machine Learning

HeLa-FUCCI cells kindly provided by Dr. Cornel Fraefel (University of Zurich) were grown on 96-well imaging plates (Greiner Biosciences), infected with HAdV-C5_wt (moi 1) in the presence of FLV (63 and 125 nM) and fixed with paraformaldehyde 18h pi. Nuclei were visualized with DAPI, and protein VI expression was used to estimate the infection efficiency [6]. Nuclear stain of DAPI was used to segment cells using Cell Profiler [2, 5, 8, 9]. Quantification of cells in different cell cycle stages was performed using Cell Profiler Analyst software and Machine Learning Algorithms [10, 11]. FUCCI plasmid in HeLa cells expresses Kusabira orange fused Cdt1 gene (mKO-Cdt1) which indicates G1 stage, and Azami Green-labeled Geminin (mAG-hGem), which indicates S/G2/M phase of cell cycle. A small gap in fluorescence change from red to green indicates a G1/S transition phase, already indicating an onset of S phase [12]. Using these set of rules, the software differentiated between G1, G1/S and S/G2/M cells. Following this, the analysis was re-examined and errors were manually corrected and software was re-trained. After several iterations, the modified training set was used for the entire data set.

Click chemistry and visualization of single viral DNA dots

HeLa-ATCC cells were grown on alcian-blue coated cover slips and infected with HAdV-C5-EdC (average bound particles per cell was 27) in the presence of FLV (15 and 60 nM) at 37˚C for 1h. Unbound virus was washed away and infection continued for 2.5h. Cells were fixed with paraformaldehyde, and processed for Copper-catalyzed azide staining as described before [13]. Virus capsids were visualized using the anti-hexon antibody Mab 9C12 (the antibody was developed by Laurence Fayadat and Wiebe Olijve, and obtained from Developmental Studies Hybridoma Bank developed under the auspices of the National Institute of Child Health and Human Development and maintained by the University of Iowa, Department of Biology, Iowa City, IA). Samples were imaged with Leica SP8 upright confocal microscope, and maximal projections were analyzed using Cell Profiler. DAPI staining was used to identify a nuclear mask, and the hexon channel (in overexposed mode) was used to segment the cell boundary. Capsid and DNA puncta over nucleus and within the cytoplasm were counted.

Virus growth assay

HCE cells were infected with HAdV-C2, D8 and D37 (moi of 0.008) at 37˚C for 2h. Cells were washed several times with PBS, and further incubated at 37˚C for 48h in growth medium containing 10% FBS. The cells were scraped and collected with medium, freeze thawed 3 three times and resultant virus titers were determined by infection of HeLa-ATCC cells with serial dilutions of the extracts and quantifying determining the number of hexon positive cells

Supporting references

[1] Araki-Sasaki, K., Ohashi, Y., Sasabe, T., Hayashi, K., Watanabe, H., Tano, Y., and Handa, H. (1995) An SV40-immortalized human corneal epithelial cell line and its characterization, *Invest Ophthalmol Vis Sci 36*, 614-621.

[2] Yakimovich, A., Gumpert, H., Burckhardt, C. J., Lutschg, V. A., Jurgeit, A., Sbalzarini, I. F., and Greber, U. F. (2012) Cell-free transmission of human adenovirus by passive mass transfer in cell culture simulated in a computer model, *J Virol 86*, 10123–10137. doi: 10.1128/JVI.01102-12.

[3] Nagel, H., Maag, S., Tassis, A., Nestle, F. O., Greber, U. F., and Hemmi, S. (2003) The alphavbeta5 integrin of hematopoietic and nonhematopoietic cells is a transduction receptor of RGD-4C fiber-modified adenoviruses, *Gene Ther 10*, 1643-1653. doi: 10.1038/sj.gt.3302058.

[4] Greber, U. F., Willetts, M., Webster, P., and Helenius, A. (1993) Stepwise dismantling of adenovirus 2 during entry into cells, *Cell 75*, 477-486. doi: 0092-8674(93)90382-Z [pii].

[5] Prasad, V., Suomalainen, M., Pennauer, M., Yakimovich, A., Andriasyan, V., Hemmi, S., and Greber, U. F. (2014) Chemical Induction of Unfolded Protein Response Enhances Cancer Cell Killing through Lytic Virus Infection, *J Virol 88*, 13086-13098. doi: 10.1128/JVI.02156-14.

[6] Burckhardt, C. J., Suomalainen, M., Schoenenberger, P., Boucke, K., Hemmi, S., and Greber, U. F. (2011) Drifting motions of the adenovirus receptor CAR and immobile integrins initiate virus uncoating and membrane lytic protein exposure, *Cell Host Microbe 10*, 105-117. doi: 10.1016/j.chom.2011.07.006.

[7] Ma, H. C., and Hearing, P. (2011) Adenovirus structural protein IIIa is involved in the serotype specificity of viral DNA packaging, *J Virol 85*, 7849-7855. doi: 10.1128/JVI.00467-11.

[8] Yakimovich, A., Andriasyan, V., Witte, R., Wang, I. H., Prasad, V., Suomalainen, M., and Greber, U. F. (2015) Plaque2.0-A High-Throughput Analysis Framework to Score Virus-Cell Transmission and Clonal Cell Expansion, *PLoS One 10*, e0138760. doi: 10.1371/journal.pone.0138760.

[9] Yakimovich, A., Yakimovich, Y., Schmid, M., Mercer, J., Sbalzarini, I. F., and Greber, U. F. (2016) Infectio: a Generic Framework for Computational Simulation of Virus Transmission between Cells, *mSphere 1*. doi: 10.1128/mSphere.00078-15.

[10] Carpenter, A. E., Jones, T. R., Lamprecht, M. R., Clarke, C., Kang, I. H., Friman, O., Guertin, D. A., Chang, J. H., Lindquist, R. A., Moffat, J., Golland, P., and Sabatini, D. M. (2006) CellProfiler: image analysis software for identifying and quantifying cell phenotypes, *Genome Biol 7*, R100. doi: 10.1186/gb-2006-7-10-r100.

[11] Carpenter, J. E., Hutchinson, J. A., Jackson, W., and Grose, C. (2008) Egress of light particles among filopodia on the surface of Varicella-Zoster virus-infected cells, *J Virol 82*, 2821-2835.

[12] Sakaue-Sawano, A., Kurokawa, H., Morimura, T., Hanyu, A., Hama, H., Osawa, H., Kashiwagi, S., Fukami, K., Miyata, T., Miyoshi, H., Imamura, T., Ogawa, M., Masai, H., and Miyawaki, A. (2008) Visualizing spatiotemporal dynamics of multicellular cell-cycle progression, *Cell 132*, 487-498. doi: 10.1016/j.cell.2007.12.033.

[13] Wang, I. H., Suomalainen, M., Andriasyan, V., Kilcher, S., Mercer, J., Neef, A., Luedtke, N. W., and Greber, U. F. (2013) Tracking viral genomes in host cells at single-molecule resolution, *Cell Host Microbe 14*, 468-480. doi: 10.1016/j.chom.2013.09.004.